UNCLASSIFIED

SECURITY CLASSIFICATION OF THIS PAGE *(When Data Entered)*

REPORT DOCUMENTATION PAGE

READ INSTRUCTIONS BEFORE COMPLETING FORM

(14) 1. REPORT NUMBER: DTNSRDC-79/089

2. GOVT ACCESSION NO.

3. RECIPIENT'S CATALOG NUMBER

(6) 4. TITLE (and Subtitle): PROJECTED GRID MOIRE TECHNIQUES FOR DEFLECTION MEASUREMENTS OF DYNAMIC APPLICATIONS

(9) 5. TYPE OF REPORT & PERIOD COVERED: Final rept.

6. PERFORMING ORG. REPORT NUMBER

(10) 7. AUTHOR(s): Jerome P. Sikora

8. CONTRACT OR GRANT NUMBER(s)

9. PERFORMING ORGANIZATION NAME AND ADDRESS
David W. Taylor Naval Ship Research and Development Center
Bethesda, Maryland 20084

10. PROGRAM ELEMENT, PROJECT, TASK AREA & WORK UNIT NUMBERS
(See reverse side)

11. CONTROLLING OFFICE NAME AND ADDRESS

(12) 36

(11) 12. REPORT DATE: Nov 1979

13. NUMBER OF PAGES: 36

14. MONITORING AGENCY NAME & ADDRESS *(if different from Controlling Office)*

(15) F61412

15. SECURITY CLASS. *(of this report)*: UNCLASSIFIED

15a. DECLASSIFICATION/DOWNGRADING SCHEDULE

16. DISTRIBUTION STATEMENT *(of this Report)*

(17) ZF61412P01

APPROVED FOR PUBLIC RELEASE: DISTRIBUTION UNLIMITED

17. DISTRIBUTION STATEMENT *(of the abstract entered in Block 20, if different from Report)*

DDC RECEIVED DEC 4 1979 A

18. SUPPLEMENTARY NOTES

19. KEY WORDS *(Continue on reverse side if necessary and identify by block number)*

Deflection Measurements
Moire
Dynamics
Propellers
Blast Response

20. ABSTRACT *(Continue on reverse side if necessary and identify by block number)*

Projected grid moire methods have potential advantages over other deflection measurement techniques because they are full-field and non-contacting. However, these techniques had not been applied to dynamic problems. Such methods have now been developed and were used to measure

(Continued on reverse side)

DD FORM 1 JAN 73 1473 EDITION OF 1 NOV 65 IS OBSOLETE S/N 0102-LF-014-6601

UNCLASSIFIED

SECURITY CLASSIFICATION OF THIS PAGE *(When Data Entered)*

397 192

(Block 10)

Program Element 62766N
Task Area ZF 614 12 001
Work Unit 1730-355

(Block 20 continued)

deflections of rotating propellers with good success and plates subject to blasts with limited success. Comparisons with analytical results show good agreement when quality photographs of the moire fringe patterns are produced.

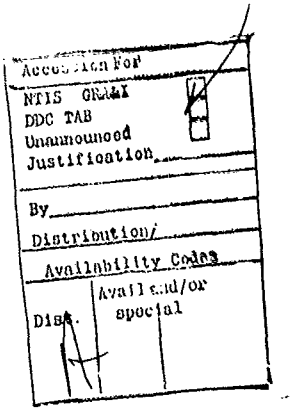

TABLE OF CONTENTS

LIST OF FIGURES

ABSTRACT

Projected grid moire methods have potential advantages over other deflection measurement techniques because they are full-field and noncontacting. However, these techniques had not been applied to dynamic problems. Such methods have now been developed and were used to measure deflections of rotating propellers with good success and plates subject to blasts with limited success. Comparisons with analytical results show good agreement when quality photographs of the moire fringe patterns are produced.

ADMINISTRATIVE INFORMATION

The results presented in this report were sponsored by the In-House Research and Exploratory Development Program of the David W. Taylor Naval Ship Research and Development Center under Program Element 62766N, Task Area ZF 614 12 001 and Work Unit 1730-355. The work was performed in the Ship Structures Division of the Structures Department during Fiscal Years 1978 and 1979.

INTRODUCTION

There is currently an increasing emphasis on the analysis of dynamic and transient responses of structures. To enhance our dynamic capability, a program was undertaken to develop suitable optical methods for measuring deflections and distortions. Optical approaches were suggested because they are full-field, noncontacting, and can often be performed on the actual object as it is being experimentally evaluated. Holographic and speckle methods have been used in the past. Although powerful tools, they are limited to small displacements and can only be taken out of a laboratory environment with great difficulty. Moire methods, although limited to larger displacements, are easier to apply in a nonlaboratory environment and do not require exotic light sources.

A promising method to measure the difference between two surfaces by a projected grid technique was first suggested by Hovanesian with others[1,2*] and later expanded by Wasowski.[3] Deflections are simply obtained by comparing the initial shape of an object with its deformed shape.

*A complete listing of references is given on page 29.

Using the above methods as a starting point, work was concentrated in two difficult problem areas: (1) blade deflection measurements on a marine propeller rotating in a water tunnel, and (2) a deflection-time history of a clamped plate subjected to an explosive air blast. The development of suitable optical techniques for these problems is presented in this report along with calculated stresses and photographs of the resulting moire fringes and deflections.

THEORY

The deflection of an object can be measured by a projected grid moire technique. Figures 1 and 2 depict a linear ruling or grid obliquely projected onto the surface of an object and photographed by a far-field camera. The point light source which projects the grid will fill the space about the object with alternating planes of light and shadows (bright or dark bands). Every point illuminated on the object, therefore, will be in a bright or dark band. If a point P_1, in Figure 2, was initially photographed in a bright band and then displaced to P_2 in a direction in line with the camera, it will be either in a bright or dark band. Constructive interference occurs when P_2 is again photographed in a bright band, while destructive interference occurs when P_2 is in a dark band. Moire fringes of destructive interference can be observed in the double exposure photograph in regions which are deflected through 1/2, 3/2, 5/2, ... bands of projected light. Constructive interference occurs at corresponding integer locations.

Referring to Figure 2, let the point light source be the origin of a polar coordinate system in a plane defined by the point light source, the camera lens, and the normal to the grid rulings.

Point P_1 was originally at (r_1,θ_1) and was deflected in the Y direction Δ, one constructive interference phase shift to P_2 at (r_2,θ_2). Hence,

$$\Delta_{1,2} = r_1 \sin \theta_1 - r_2 \sin \theta_2 \qquad (1)$$

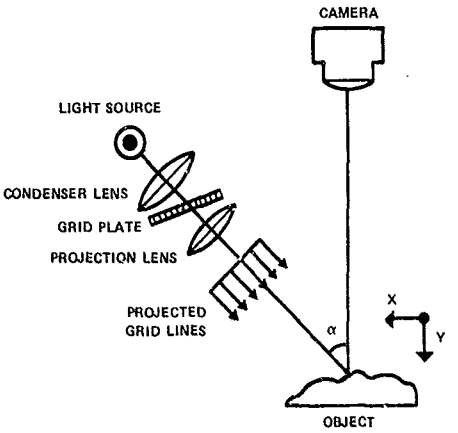

Figure 1 - Optical Arrangement to Measure Deflections in Y-Direction

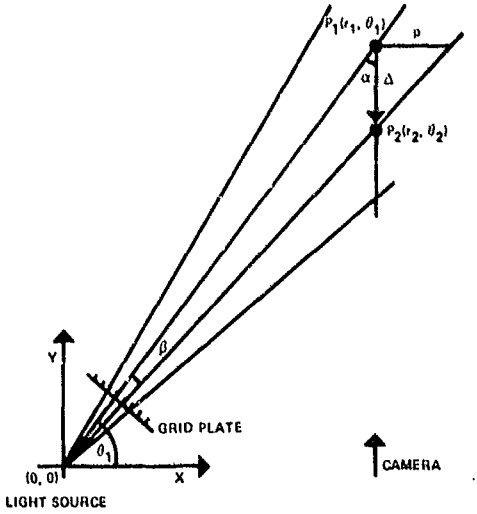

Figure 2 - Schematic of Optical Setup for Single Light Source

Since $r_2 = r_1 \cos\theta_1/\cos\theta_2$, and the angle β, subtended by adjacent planes, is the difference between θ_1 and θ_2, it can be shown that

$$\Delta_{1,2} = \frac{r_1}{\cos\theta_2}(\sin\theta_1\cos\theta_2 - \cos\theta_1\sin\theta_2)$$

$$= \frac{r_1 \sin(\theta_1-\theta_2)}{\cos\theta_2}$$

$$= \frac{r_1 \sin\beta}{\cos(\theta_1-\beta)} \qquad (2)$$

Furthermore, the total deflection through two constructive interference fringes would be

$$\Delta_{1,3} = \frac{r_1 \sin 2\beta}{\cos(\theta_1-2\beta)}$$

and, in general,

$$\Delta_{1,n+1} = \frac{r_1 \sin(\mp n\beta)}{\cos(\theta_1 \mp n\beta)} \qquad (3)$$

where $+n$ (the number of interference fringes) is toward the camera and $-n$ is away from the camera. From Equation (3), the distance $\Delta_{n,n+1}$, between successive interference fringes is not constant. However, in practice, r_1 is generally large and β is small so the difference between successive fringes is often small.

For a far-field camera, the surface of the object can be assumed to lie in a plane. Thus, the distance p of Figure 2 can be related to the deflection Δ by

$$\Delta_{1,2} = \frac{p}{\tan(\alpha+\beta)} \tag{4}$$

In general, when β is small or the projected light is collimated ($\beta \equiv 0$), Equation (4) reduces to

$$\Delta_{1,n+1} = \frac{np}{\tan \alpha} \tag{5}$$

which is equivalent to Hovanesian's et al.[1,2] results from light intensity considerations. The intensity distribution on the film plate is

$$I_1(X,Z) = k\left[1+ \sin \frac{2\pi}{p} (X-Y_1 \tan \alpha)\right] \tag{6}$$

where $Y_1 = f(X,Z)$ surface of object

k = constant

Z = normal to the X-Y plane

If the object undergoes a normal (Y direction) displacement, the intensity distribution $I_2(X,Z)$ occurs which is similar to that of Equation (6) except that Y_1 is replaced by $Y_1 + \Delta = Y_2$. If a double-exposure photograph is made, the resulting intensity distribution on the film is given by

$$I_1 + I_2 = 2k\left[1+ \sin\left(\frac{\pi}{p}\left[2X-(Y_1+Y_2)\tan \alpha\right]\right) \cos\left(\frac{\pi\Delta}{p} \tan \alpha\right)\right] \tag{7}$$

Equation (2) is a case of a high frequency carrier term being amplitude modulated by a lower frequency term. Moire fringes occur when the high frequency term (the cosine term) is completely nulled,

$$\Delta = \frac{np}{\tan \alpha} \tag{8}$$

$$\pm n = 1/2,\ 3/2,\ 5/2,\ \ldots$$

Each Moire fringe is a contour of normal displacement, and successive fringes are equal increments apart.

An alternative to making double-exposure photographs is to make a negative of the projected grid on the undeformed surface. Similarly, a second negative of the deformed surface is also made and the two negatives can be superimposed as a sandwich. Moire fringes, as in the double-exposure method, will be observed. This method is analogous to that of sandwich holography. To avoid in-plane rotational errors and lateral translations in this technique, it is helpful to include a second object in the scene which is not deformed so that markings on the second object can be accurately superimposed.

A contour map of the object can be similarly obtained by comparing the surface of the object with a plane. A variation of the arrangement from Reference 1 is shown in Figure 3. Partial mirrors are placed in the path of the camera and projection system so that a reference plane can be seen superimposed on the object. The reference plane must be positioned such that the distance from mirror (1) to the object equals the distance from

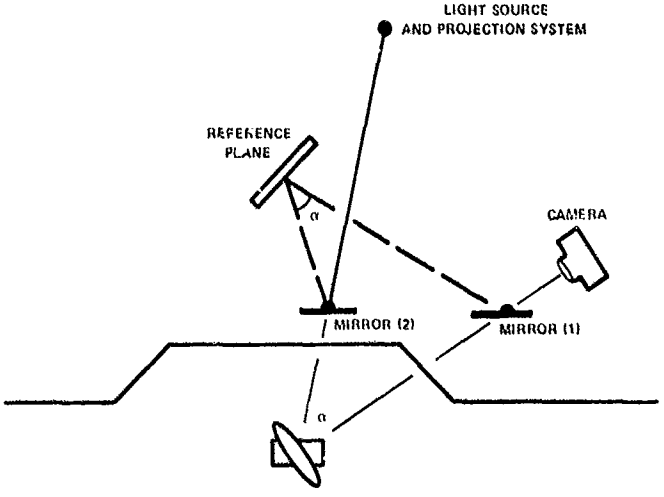

Figure 3 - Schematic for Contour Difference Setup

mirror (1) to the reference plane. Mirror (2) must also be equidistant from the object and reference plane. Under these conditions, the projected fringes on the object will interfere with those on the reference plane producing a contour-difference map which can be evaluated by Equation (3). A left-to-right reversal of the reference plane is induced by the mirrors. This limits the method to comparing the object with plane or mirror-symmetric surfaces and requires that the projected grid lines be of constant pitch everywhere on the surface. Although the use of partial mirrors permits the contour fringes to be seen in real time or photographed with a single exposure, the system is not very light efficient for dynamic applications. A double exposure variation can be employed with standard mirrors which are removed between exposures. The contrast of the interference fringes can be further improved by separate film plates for each exposure and then superimposing (or sandwiching) the negative. With a judicious choice of projected grid lines, one can substitute the negative of the reference plane with a high quality master grid, further improving the contrast of the interference fringes.

Another real-time contour map of the object's surface can be generated by using two projectors inclined at angles about the camera, see Figure 4. For simplicity, let each projector be at the same angle α relative to the camera and align the projected rulings so that they are parallel to each other. From Figure 4, the space about the object is filled with surfaces of constructive and destructive interference. Wasowski[3] has shown that these surfaces form elliptic or hyperbolic cylinders. Hence, a plane object will have moire fringes on it. The distance between points P_1 and P_2 of Figure 4 corresponds to two interference fringes being formed. Thus, twice as many moire fringes will appear in the dual projector method as in the single projector case of Figure 2. Equations (3) and (5) may be used where $n = \pm 1/2, 1, 3/2, 2, 5/2, \ldots$ at increments of constructive interference.

The drawback of having contours of elliptic or hyperbolic cylinders rather than planes can be overcome by using collimated light projectors or by using homomorphic grids, grids with linearly varying rulings.

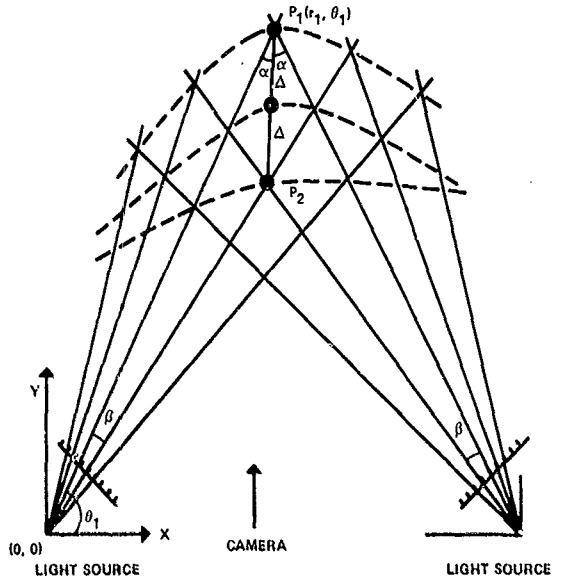

Figure 4 - Schematic of Optical Setup for Dual Light Source

Collimated systems limit the size of the object which can be studied. Whereas, homomorphic grids are more difficult to obtain and align than are standard grids.

The sensitivity of all of the methods are a function of the pitch of the grid and of the angle between the projector and the camera. The high frequency carrier (projected grid lines) becomes unresolvable by the eye or film when p becomes too small. Problems may also be encountered when the projector is at too large an angle α to the normal of the object's surface. In previous work, conventional slide or viewgraph projectors were used to illuminate the object; however, as the angle α increased, it was not

possible to focus the grid on all parts of the surface at the same time. An open projection system, see Figure 1, therefore, was constructed for this study by placing a condenser lens in front of an appropriate light source (either flash or conventional lamp). The grid, usually on a glass plate to avoid distortions, is placed close to the condenser to assure maximum and uniform illumination. A projection lens then focuses the image onto the object. A telephoto camera lens was found to be superior to conventional projector lenses. The grid was focused on all parts of the object's surface by rotating the grid plate (and sometimes the projection lens).

The camera viewing the object should be nearly in line with the direction of normal displacement. If the camera is at too great an angle, or if there is a relatively large in-plane displacement, two distinct images (one from each exposure) will be seen on the resulting photograph. This effect generally limits the techniques to bending problems or to normal translations.

DEFLECTION ANALYSIS OF ROTATING PROPELLERS

A considerable effort has been invested in the structural analysis of marine propeller blades. The combined centrifugal and dynamic pressure loads cause the propeller's blades to deflect which may cause additional changes in the pressure distribution on the blade. The effects of a ship's wake and fluctuations in flow patterns present even more problems for the propeller analyst.

An experimental approach to measure the stresses and deflections of propellers operating under water would be beneficial. Strain gages may be used on operating propellers, but the gage installation on the blade surface may affect the flow patterns or alter blade response if the gages are recessed. Furthermore, the number of gages is usually limited because of difficulties in transferring the gage signal from the blade. A holographic approach[4,5] has achieved some limited success, but, the sensitivity of holography is a disadvantage in the churning, vibrating,

hostile environment of a water tunnel or open channel. Although projected grid techniques are much less sensitive than holography, they are also less disturbed by hostile environments.

As a first step toward measuring the deflections of a propeller rotating in a water tunnel, deflections of a propeller rotating in air were performed. A plastic, rectangular blade, 254 mm (10 in.) diameter × 25 mm (1 in.) × 3 mm (1/8 in.) with eccentric masses 12 mm (1/2 in.) from the blade tips, was rotated at speeds up to 900 rpm by a d.c. motor. Figure 5 shows the experimental setup. A laser beam was reflected from a mirror on the motor shaft onto a photodetector 4.3 m (14 ft) away. The photodetector triggered a flash strobe which projected a grid of 1.46 lines/mm (37 lines/in.) onto the rotating blade when it was in the desired angular position. The first exposure was made while the blade rotated slowly. The blade speed was then increased and the photodetector advanced so the second exposure would occur with the blade in the same angular position. Photographs of the moire fringes on the blade at 480 and 756 rpm are shown in Figure 6. The displacements along the centerline of the blade were measured and are plotted in Figure 7 along with those from a finite element analysis.* A power function was fit by least squares to the displacements at each speed. Strains and stresses were then calculated from the second derivative of the functions and are plotted in Figure 8 along with those from the finite element analysis.

Thus, having established the validity of the technique for rotating objects, a three-bladed, left-handed, 24.4 cm (9.6 in.) diameter, aluminum, marine propeller (Figure 9) was mounted in the 0.9 m (36 in.) variable pressure water tunnel at DTNSRDC. Figures 10 and 11 show the optical setup at the water tunnel and a schematic view, respectively. A flash strobe projected a grid of 0.53 lines/mm (13.5 lines/in.) onto the propeller through one of the side viewing ports of the water tunnel. A camera was mounted to photograph the propeller through one of the small oblique viewing ports. Because of the fixed position of the oblique ports and the location of the tunnel nozzle, the entire surface of one of the blades could not be photographed while the blade was normal to the camera. An

*The finite element analysis was provided by Dr. J. Adamchak.

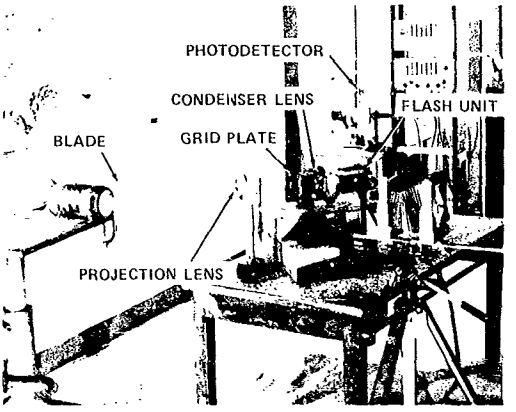

Figure 5 - Experimental Setup for Propeller Rotating in Air

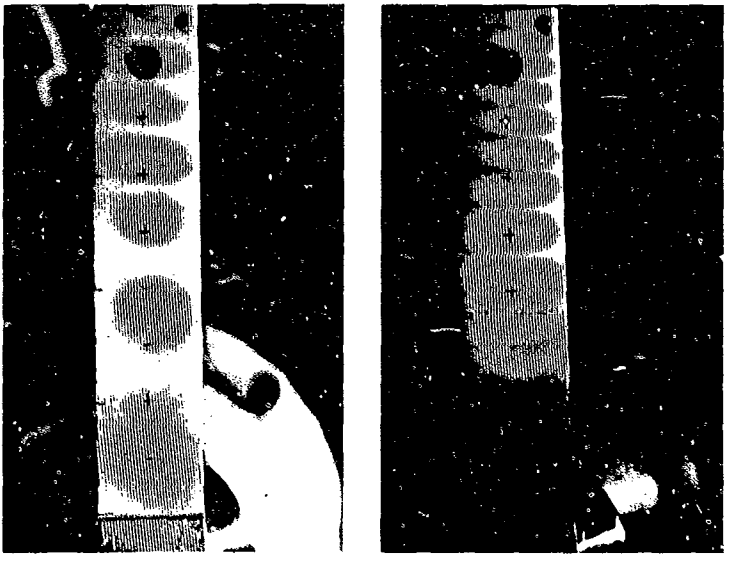

Figure 6 - Deflection Fringes on Propeller Rotating in Air

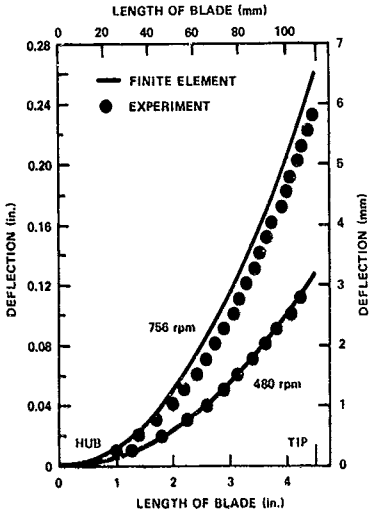

Figure 7 - Blade Deflections of Propeller in Air

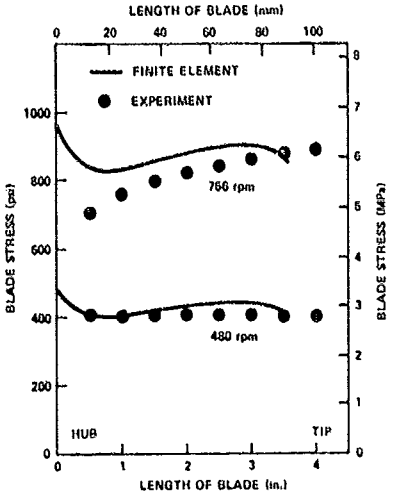

Figure 8 - Blade Stresses of Propeller in Air

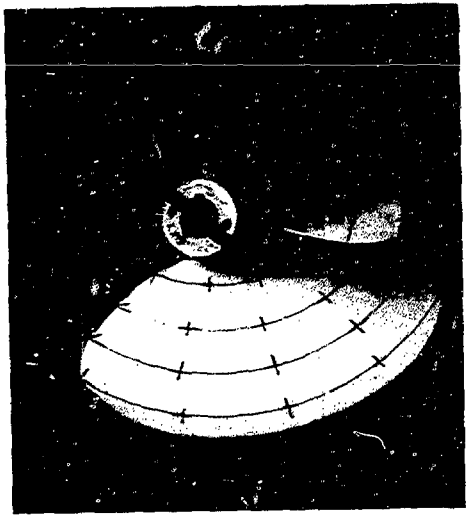

Figure 9 - Marine Propeller

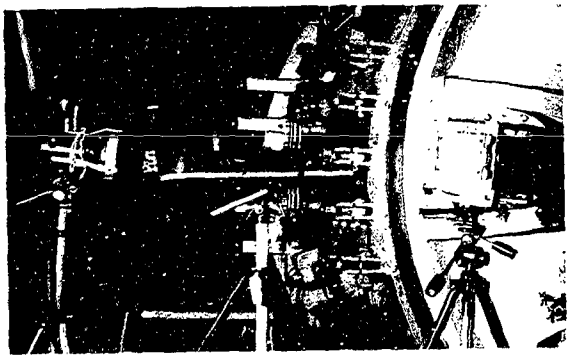

Figure 10a - Apparatus Outside Tunnel

Figure 10b - Propeller Inside Tunnel

Figure 10 - Experimental Setup at the 36-Inch Water Tunnel

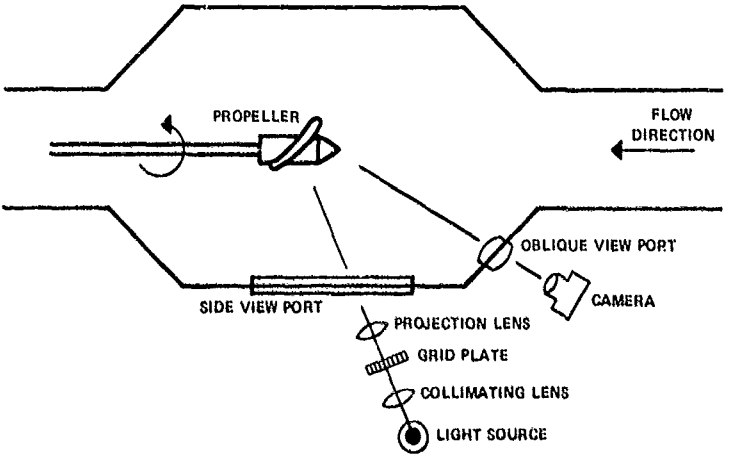

Figure 11 - Schematic of Optical Setup at the Water Tunnel

available magnetic pickup on the propeller shaft was used to trigger the flash strobe when the propeller was in the desired angular positions. Photographs of the moire deflection fringes on the propeller rotating at 1000 rpm under water are shown in Figure 12. The blade was loaded by varying the flow velocity (up to 15 m/s (50 ft/sec)) in the tunnel between the two exposures. This corresponds to the crash ahead and crash astern load conditions with the thrust loads on the propeller reaching 4900 N (1100 lb). Figure 13 is a plot of blade deflections along the midchord radius line. Difficulties with the triggering device precluded varying the rotational speed of the propeller while maintaining the flash at the same angular position as in the case in air. Double-exposure photographs made of the propeller rotating at 500 and 2000 rpm showed obvious rotational nonsynchronization effects.

The shape of the propeller was measured by the previously described contour difference method which is depicted in Figure 3. Photographs of the propeller rotating in the water tunnel were unfortunately underexposed. Figure 14 is, however, a photograph of the contour fringes on the propeller at rest. Since the shape of the propeller relative to a plane involves greater distances than the deflections, a coarser projected grid was employed resulting in interference fringes of sharp contrast.

DEFLECTION ANALYSIS OF EXPLOSIVELY LOADED PLATES

The determination of the response of structures subject to explosive blasts is important for the development of accurate predictions of ship damage. Strain gages and pressure gages have been used in attempts to determine the responses of structures. However, difficulties may arise when such instrumentation is subject to the high accelerations encountered in the shock wave of an explosion. Therefore, a noncontacting projected moire method was pursued to obtain a deflection time-history of plates in a shock blast.

To obtain an understanding of the damage mechanism associated with confined explosions, Zilliacus et al.,[6] constructed a chamber for testing a simple plate model. Their test chamber was used in this study. The chamber was welded to a deep I-beam which, in turn, was welded to the floor of the explosion test pit at DTNSRDC; see Figure 15. A 30 cm (12 in.)

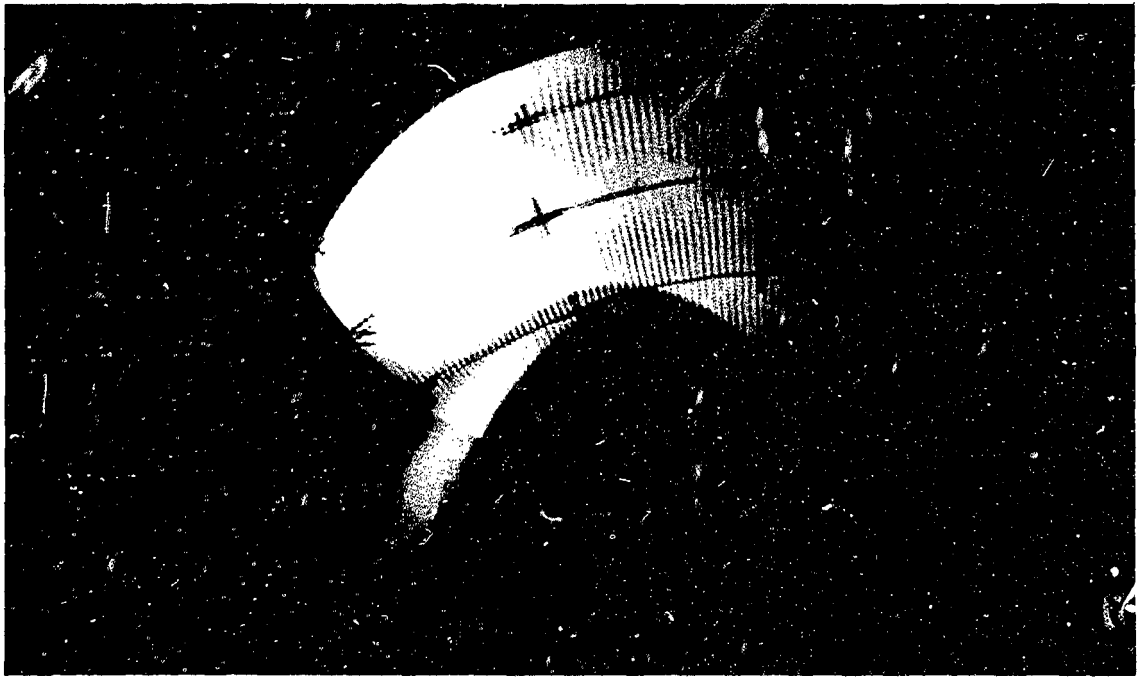

Figure 12 - Deflection Fringes on Propeller Rotating Under Water

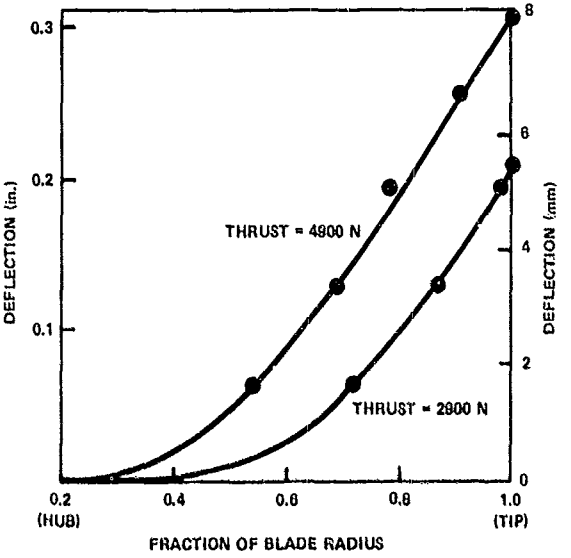

Figure 13 - Blade Deflections of Propeller Rotating Under Water

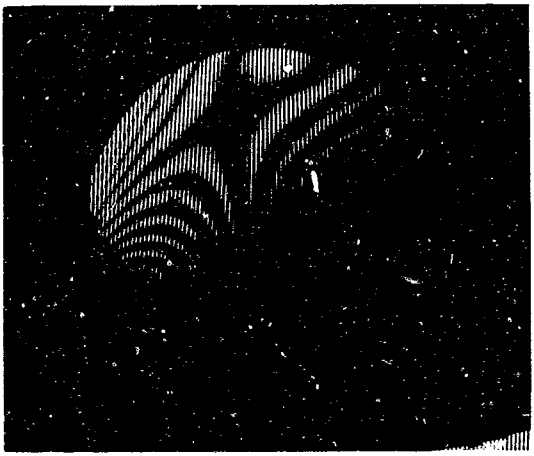

Figure 14 - Contour-Difference Fringes on Propeller Blade

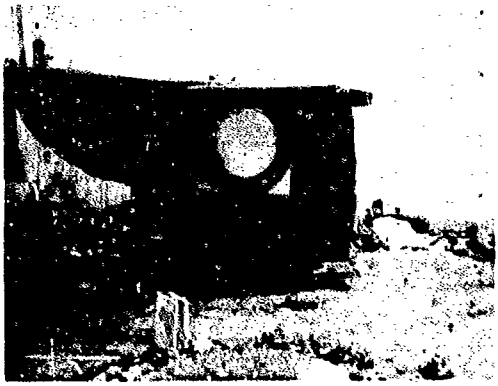

Figure 15 - Explosion Cylinder in Test Pit

diameter circular plate was bolted by a restraining ring to the end of the cylindrical explosion chamber. An explosive charge was mounted to the wall at the back end of the chamber. The tests employed 3 mm (0.125 in.) thick aluminum plates loaded by 3 g charges of Pentolite at a standoff distance of 50 cm (16 in.). This caused the plates to permanently deform up to 33 mm (1.3 in.) at the center. Figure 16 is a photograph of one of the deformed plates. Small holes or rips often occurred near the centers of the plates which were possibly caused by fragments of the detonator.

Three optical arrangements were evaluated in the test pit. The single light source method of Figure 2 was first employed. Grid lines with a pitch of 0.2 lines/mm (5 lines/in.) were projected onto the plate by a floodlamp while being photographed by a movie camera at a rate of 100 frames/sec. The film was rewound for the second exposure so that the frames lined up. A shift in the images of each exposure by a distance corresponding to an integral number of film sprocket holes was easily avoided by the use of 16 mm film which has one sprocket hole per frame (8 mm film can also be used, but the smaller format is a distinct disadvantage for resolving the projected grid lines on the plate). The camera was then run at 10,000 frames/sec while the flashbulb and explosive charge were consecutively detonated. Although interference fringes could be distinguished in the movies, the contrast was not sufficient to permit reproduction. An example of the fringe pattern is shown in Figure 17 which is a static photograph using the contour-difference method on the plate after it had deformed.

The second arrangement was the dual light source method of Figure 4. A single exposure of the movie film was made at a rate of 10,000 frames/sec while flashbulbs simultaneously projected grid lines from two directions as the charge was detonated. Unfortunately, the films were again of insufficient quality to reproduce.

The third arrangement used the shadow moire method described by Meadows et al.[7] and Takasaki.[8] A grid of 1.18 lines/mm (30 lines/in.) was held at a distance of 30 mm (1.25 in.) in front of and parallel to the plate. A single exposure of the movie film was made at a rate of 10,000

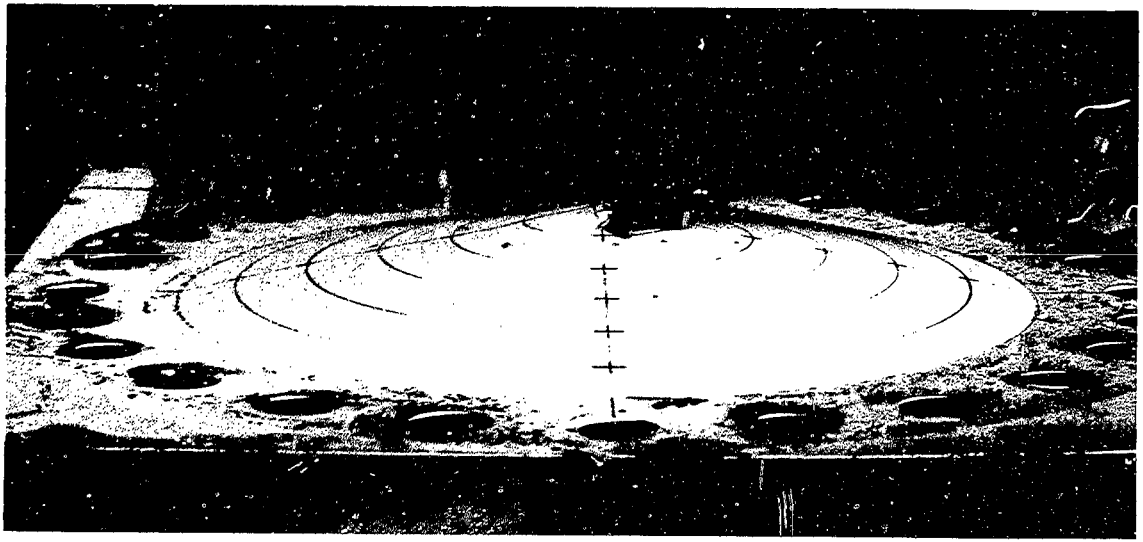

Figure 16 - Plate Deformed by Explosive Blast

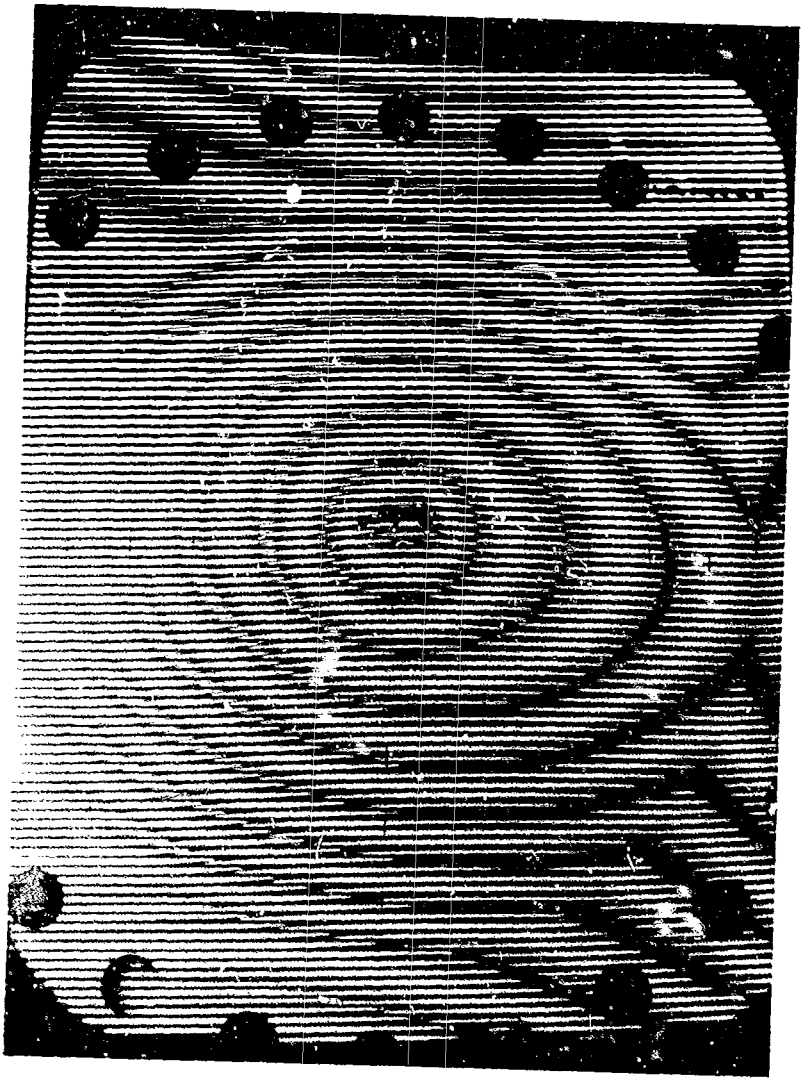

Figure 17 - Contour-Difference Fringes on Plate

frames/sec while flashbulbs illuminated the plate from an oblique direction as the charge was detonated. The light directed through the grid produced shadows on the surface of the plate. As the plate deformed, the shadows and the grid itself interfered to form moire contour fringes of the plate. Admittedly not of high contrast, Figure 18 is a photograph of the shadow moire fringes from the high speed film. Figure 19 shows shadow moire fringes on the plate after it was deformed and removed from the explosion chamber. The good quality photograph of Figure 19 was made with a large format (4×5) camera rather than reproducing the 16 mm movie film of Figure 18. The permanent deflections on the plate were determined from Figure 19 and are presented in Figure 20.

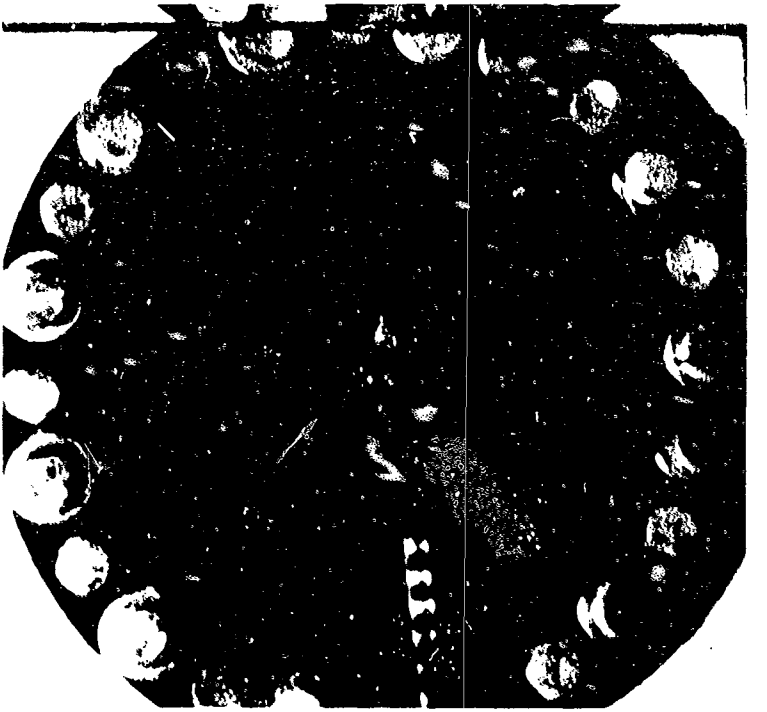

Figure 18 - Shadow Moire Fringes from High Speed Movies

Figure 19 - Shadow Moire Deflection Fringes on Plate

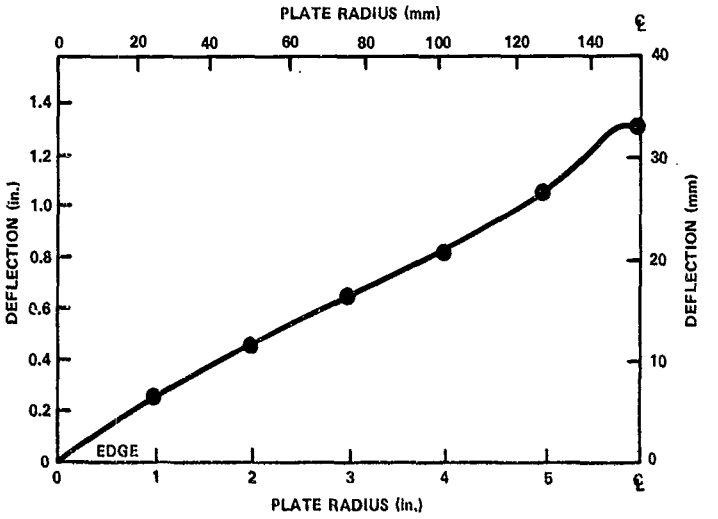

Figure 20 - Deflection Along Radial Direction of Plate

DISCUSSION OF RESULTS

The resolution of the projected grid method is a function of the size of the object and the size of the image on the film. The common photographic films used in this study were able to resolve at least 20 lines/mm (500 lines/in.) of the film image. Since high contrast of the projected grid lines on the object produced the best quality moire fringes, high contrast films were evaluated and were found to produce the best results. The contrast of the projected grid lines became poor when the product of the object diameter (mm) and the projected line spacing (lines/mm) exceeded 300. Thus, an object with a 600 mm (2 ft) diameter should be illuminated by a source with a projected line spacing of 0.5 lines/mm (12.5 lines/in.). Assuming an illumination angle α of 45 deg, five observed fringes correspond to a displacement of 10 mm (0.4 in.). Similarly, an object with a 25 mm (1 in.) diameter can be illuminated by

a source with a projected line spacing of 12 lines/mm (300 lines/in.) corresponding to a displacement, at five fringes, of 0.2 mm (0.008 in.). The smallest film size that could be used is 35 mm for the first case and 50 mm for the second. Larger film sizes, with larger images, are preferable however.

The accuracy of the method can be determined from counting the number of moire fringes plus or minus about a sixth or eighth of a fringe. For a two percent accuracy, one should have seven or eight moire fringes. This is shown by the good agreement of the experimental results of the propeller rotating in air at 480 rpm (Figure 7) with the finite element analysis. The displacements at 756 rpm are consistently low, not because of the accuracy of the method, but because the displacements are so large (twice the thickness) that the linear assumptions of the finite element analysis are not strictly valid.

The good quality of the photographs showing the moire interference fringes demonstrates the feasibility of using such techniques to measure deflections on rotating propellers in a water tunnel environment. Vibrations of the shaft and tunnel as well as particles and entrapped air were not found to be detrimental. The simplicity of the method in obtaining full-field deflections is a prime advantage of this technique in solving a most difficult experimental problem.

Future water tunnel tests involve additional considerations. More fringes would have been observed in Figure 12 if a finer grid had been projected onto the propeller. Although the high contrast film could resolve finer projected grid lines, it was difficult to focus them on the blade using the strobe light as a light source. A more rigid optical stand which would permit interchanging the strobe light with a flood light for alignment purposes is required. Because of the curvature and varying pitch of the propeller, not all parts of the blade deflected in line with the camera. This, together with the fixed position of the camera due to the viewing ports, results in the dual images seen along the trailing edge of the blade in Figure 12. Although the viewing port diagonally across the tunnel had a somewhat better view, cavitation bubbles obscured

that face of the blade. (Cavitation bubbles can also be seen trailing from the silhouetted blade in the foreground of Figure 12.) The method would be most useful on a propeller of uniform pitch provided the camera could view in a normal direction to the pitch angle. Since most propellers have a low pitch angle, a direct viewing port or an indirect system of prisms or mirrors should ideally be located as close to the flow direction as possible without obstructing the flow.

Improvements in high speed motion pictures of a plate deforming by an explosive blast involve the following parameters. Unless the slow speed first exposure and the high speed second exposure are of equal intensity, the interference fringes will be of poor quality. This is the most likely cause for the poor results obtained. It is also necessary to reduce the ambient light as much as possible. The choice in resolution and contrast in film is very limited. The relatively large deflection fortunately permits the use of coarse grids. The most critical parameter is using a frame rate sufficiently fast to capture the event being studied. Since the fastest 16 mm camera available at the time of the study was limited to 10,000 frames/sec, only a few frames could catch the plate as it deformed. The 100,000 frames/sec camera, in use elsewhere, would be an improvement in capturing the event. However, at faster film rates the electronic synchronization of bringing the camera up to speed followed by detonating the flashbulbs followed closely by detonating the charge becomes more difficult. The faster film rates also require more light, using several flashbulbs.

An optical method for predicting the stresses was suggested by Liang et al.[9]. A single exposure negative of the deformed object (with the projected grid lines) is made along with a transparent positive. The negative and positive are superimposed and rotated 180 deg apart at a point of interest. A series of ellipses or hyperbolas are formed which are proportional to the principal strains. The major disadvantage is the sensitivity of the method to small variations in the pitch of the projected grid lines. A change in pitch on the rotating blade of 5 percent produced a fictitious strain ten times that of the measured

strain. Unless a large curvature is present on the object so that the ellipses or hyperbolas form in the immediate vicinity of the point of interest, unacceptably large errors can result.

CONCLUSIONS

Deflections were measured on structures subject to dynamic and transient loadings using projected grid moire techniques. High speed motion pictures were used in an attempt to determine deflections on a circular plate subjected to an explosive air blast. Although some limited success was achieved, additional work is required to demonstrate the practicality of the method. Deflections were also measured on propellers rotating in air and under water. The fine quality of the photographs of the moire fringes demonstrates the feasibility of this method. Good agreement with analytical results confirms the accuracy of the method.

Advantages of the method include being full-field and noncontacting, requiring no special surface preparation or materials, and being able to be used in hostile environments, e.g., underwater, in high temperatures, in the vicinity of air blasts. If good quality photographs, either motion picture or flash, can be made of the structure during its loading, then a deflection analysis can be performed. As in any experimental endeavor, limitations due to timing synchronization, light intensity, photographic resolution, and physical accessibility must always be considered.

ACKNOWLEDGMENTS

Many people at the Center provided invaluable support. Barry L. Zimmerman provided the electronic synchronization for the explosive and water tunnel tests. Donnie L. Hill handled the photography of the propellers and Elzy E. McCrossin ran the high speed camera in the explosion test pit. Louis A. Becker and his crew handled the explosive charges. The entire crew at the 36-inch water tunnel were most helpful in the authors first use of that facility.

REFERENCES

1. Hovanesian Der, J. and Y.Y. Hung, "Moire Contour-Sum Contour-Difference, and Vibration Analysis of Arbitrary Objects," Applied Optics, Vol. 10, No. 12 (1971).

2. Hovanesian Der, J. et al., "Use of a Projected-Ruling Moire Method for Vibration and Deflection Measurements of Three-Dimensional Structures," Proceedings of the Symposium-Engineering Applications of Holography, Los Angeles, Calif. (1972).

3. Wasowski, J.J., "Moire Surface Contouring by Addition Method," Proceedings of the Sixth International Conference on Experimental Stress Analysis, Munich, West Germany (1978).

4. Sikora, J.P., "Structural Analysis of Propellers Rotating Under Water Using Holography," Proceedings of the SNAME Symposium-Propellers' 75, Philadelphia, Pa. (1976).

5. Sikora, J.P. et al., "Deflection, Stress, and Vibration Analysis of Rotating Propellers Using Holography," DTNSRDC Report 4507 (1974).

6. Zilliacus, S. et al., "The Response of Clamped Circular Plates to Confined Explosive Loadings," DTNSRDC Report 3987 (1974).

7. Meadows, D.M. et al., "Generation of Surface Contours by Moire Patterns," Applied Optics, Vol. 9, No. 4 (1970).

8. Takasaki, H., "Moire Topography," Applied Optics, Vol. 9, No. 6 (1970).

9. Liang, C.Y. et al., "Direct Determination of Flexural Strains in Plates Using Projected Gratings," Proceedings of the Sixth International Conference on Experimental Stress Analysis, Munich, West Germany (1978).

INITIAL DISTRIBUTION

Copies		Copies	
1	DDR&E Lib	1	NSF Engr Div Lib
1	CNO OP 098T	1	Library of Congress
1	CHONR Code 474	1	Oakland Univ. School of Eng. Rochester MI
1	DNL	1	United Tech. Res. Cntr. Instrumentation Lab.
2	NAVMAT 1 MAT 08T23 1 Lib		
2	NRL 1 Code 8431 1 Tech Lib		
1	USNA		
1	NAVPGSCOL		
1	NWC		
1	NADC		
1	NOSC Code 6342		
11	NAVSEA 1 SEA 03 1 SEA 03C 1 SEA 03D 1 SEA 035 1 SEA 05R 1 SEA 06D 1 SEA 312 1 SEA 32 1 SEA 323 1 SEA 62R 1 SEA 996		
12	DTIC		
1	Wright-Patterson AFT AFFDL-FBEC		

CENTER DISTRIBUTION

Copies	Code	Name
1	012	
1	15	
1	1503	
1	152	
1	154	
1	1544	
1	17	
1	1702	
1	1706 (m)	
1	1720	
10	1730	
1	1740	
1	1750	
1	1770	
1	1770.7 (m)	
1	1844	
1	19	
1	274	

Copies	Code	Name
1	296	
10	5211.1	Reports Distribution
1	522.1	Unclassified Lib (C)
1	522.2	Unclassified Lib (A)

GPO 881 679